Journal of Applied Polymer Science

Synthesis of aminated glycidyl methacrylate grafted rice husk and investigation of its anion-adsorption properties

Tatek Temesgen,[1] Hyunju Park,[2] Choonki Na[3]

[1]Department of Civil and Environmental Engineering, Seoul National University, 599 Gwanak-Ro, Gwanak-Gu, Seoul 151-744, South Korea

[2]Engineering Institute, Seoul National University, 599 Gwanak-Ro, Gwanak-Gu, Seoul 151-744, South Korea

[3]Department of Environmental Engineering, Mokpo National University, Jeonnam 534-729, South Korea

Correspondence to: H. Park (E-mail: narjjis@naver.com)

ABSTRACT: In this study, we focused on the synthesis, characterization, and adsorption capacity testing of aminated glycidyl methacrylate grafted rice husk (RH-*g*-GMA–Am). Our goal was to obtain a high-performance surface for the adsorption of various anions. Glycidyl methacrylate grafted rice husk (RH-*g*-GMA) was prepared by the graft copolymerization of glycidyl methacrylate with rice husk; the product was further subjected to an amination reaction. The surface properties, sorption characteristic functional groups, isotherm and kinetic studies, pore diffusion models, and effects of the temperature and pH on the material properties were studied under batch conditions. The IR spectroscopy results show additional surface functional groups for RH-*g*-GMA–Am. The adsorptions of PO_4^{3-} and NO_3^- on RH-*g*-GMA–Am were found to follow pseudo-second-order kinetics; this indicated a possible dominant role played by chemisorption. The rate-limiting step for mass transfer was found to be boundary layer diffusion. Furthermore, the sorption isotherms for NO_3^- and PO_4^{3-} fit the Langmuir model. The amination of RH-*g*-GMA drastically increased the removal efficiency from 3 to 82% and from 6 to 93% for NO_3^- and PO_4^{3-}, respectively. Moreover, RH-*g*-GMA–Am exhibited a better PO_4^{3-} removal efficiency in the pH range of 4–6.5. Regeneration studies revealed that the surface of RH-*g*-GMA–Am could be regenerated repetitively by simple acid washing with an insignificant decrease in the active surface for consecutive adsorptions. © 2015 Wiley Periodicals, Inc. J. Appl. Polym. Sci. **2016**, *133*, 43002.

KEYWORDS: addition polymerization; adsorption; grafting

Received 10 July 2015; accepted 24 September 2015

DOI: 10.1002/app.43002

INTRODUCTION

Phosphates (PO_4^{3-}) and nitrates (NO_3^-) are major nutrients required for the growth of living things. However, surface and ground water eutrophication, because of the elevated concentrations of these ions, is a current environmental concern.[1–3] Among the various PO_4^{3-} and NO_3^- removal technologies available, adsorption is a simple, effective, and inexpensive method.[3–7]

In recent years, there has been a pronounced tendency to use mechanically stable synthetic or natural solid matrices in many engineering applications. Moreover, numerous surface activation approaches have been studied to develop cheaper and more active surfaces used for applications in separation technologies, such as adsorption, which depend on active surfaces.[4,7,8]

Polymer grafting is a technique that is often applied for the development of selective surfaces with well-controlled characteristics and size distribution in adsorption applications. The new starting synthesis materials needed to develop new adsorbents with improved physicochemical properties have become scarce. In this respect, polymer grafting provides an alternative approach and has become a research focus.[5,9–11] Amination of polymer grafting improves the active functional groups of surfaces and has been explored on various surfaces for improving their anion-exchange properties.[1]

Limited investigations have been conducted on polymer grafting with glycidyl methacrylate (GMA) as a monomer. Song *et al.*[11] reported the grafting of a variety of thiol–epoxy functional groups onto polystyrene divinylbenzene glycidyl methacrylate and observed an increased surface charge because of the high surface grafting density of 2-aminoethanethiol and thioglycolic

Additional Supporting Information may be found in the online version of this article.

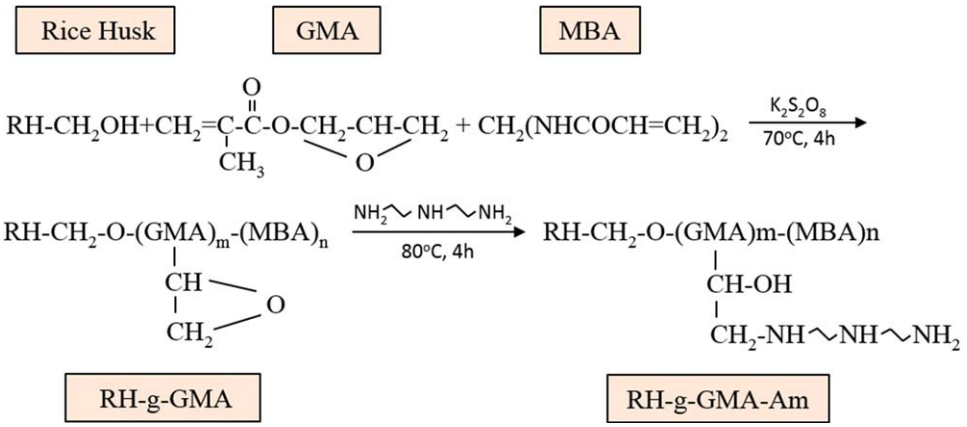

Figure 1. Schematic illustration of the preparation process and chemical structure of RH-*g*-GMA–Am. [Color figure can be viewed in the online issue, which is available at wileyonlinelibrary.com.]

acid. Furthermore, the adsorption isotherms of acid orange and toluidine blue were found to fit the Langmuir model. Gao *et al.*[12] also grafted polyethyleneimine (PEI) on the surface of the terpolymer of GMA, acrylamide (AM) and *N*, *N*′-methylene bisacrylamide microbeads (GMA/AM/MBA) and reported on the properties of the modified surface for the adsorption of bilirubin. Yang *et al.*[13] conducted a study on the adsorption of phenol on aminated activated carbon and observed an enhanced adsorption capacity. They found that the adsorption process followed the pseudo-second-order kinetic model, where the rate-controlling step was intraparticle diffusion. Furthermore, Pan *et al.*[14] studied the amination of hypercrosslinked polymeric adsorbents for the purpose of phenol adsorption and found that the amino group in the polymeric matrix played a significant role in the adsorption of phenol. They also found that the increase in the adsorption capacity was due to hydrogen-bonding interactions between the amino groups and the adsorbate molecules.

In parallel, the use of agricultural leftovers, such as rice husk (RH), for the adsorption of both organic and inorganic compounds is attracting attention because of the low cost and good performance of such materials.[1,6,7,15–17] In this study, a relatively cheap and versatile adsorbent was developed by the grafting of GMA onto RH. The surface of glycidyl methacrylate grafted rice husk (RH-*g*-GMA) was modified with an amination reaction to achieve improved adsorption of NO_3^- and PO_4^{3-}. Because RH is an abundant low-cost material with good mechanical strength and because it has a high proportion of cellulose along with other functional groups, such as hydroxyl groups,[6,17] it is suitable for use as a base material in the preparation of an adsorbent by amination. In this study, GMA (>98%) was selected as a monomer to use its vinyl and epoxide groups, which exhibit a high reactivity toward amine groups.[18] The prepared aminated glycidyl methacrylate grafted rice husk (RH-*g*-GMA–Am) adsorbent was tested in the batch configuration for the adsorption of NO_3^- and PO_4^{3-}, and the effects of the pH on the adsorption properties were examined. The adsorption isotherms and kinetics were predicted by comparison with existing modeling equations. To the best of our knowledge, the synthesis of RH-*g*-GMA–Am for applications in the removal of NO_3^- and PO_4^{3-} has not been reported in the literature.

EXPERIMENTAL

Materials

RH was provided by a local rice-milling plant. GMA (>98%, Junsei, Japan), MBA (Sigma-Aldrich), potassium persulfate ($K_2S_2O_8$; analytical-reagent grade), and cyclohexane were used as the monomer, crosslinker, initiator, and solvent, respectively. Diethylenetriamine (DETA; 97%, Daejung Chemical Co., Korea), ethylenediamine (EDA; 97%, Daejung), dimethylamine (DMA; 40% in H_2O, Sigma-Aldrich), and trimethylamine (TMA; 30% in H_2O, Yakuri, Japan) were used as amination reagents. All of the reagents were used as received.

NaF, $NaNO_2$, $NaNO_3$, Na_2HPO_4, and Na_2SO_4 were used to prepare the anion solutions used in the adsorption studies. The working solutions were prepared by the dissolution of the chemicals in deionized water with a pH buffer solution. The pH buffer solutions were composed of CH_3COOH and CH_3COONa, with a total acetate concentration of 0.01*M* at a pH of 4.7. Commercial anion-exchange resins, SAR10 [$—N^+(CH_3)_3Cl^-$; Samyang Co., Korea] and WA30 resin [$(CH_2)_nN^+(CH_3)_2OH^-$; Samyang], which are strong base and weak base anion exchangers, respectively, were used in comparative studies.

Preparation of the Aminated RH sorbent

RH was crushed and sieved to yield a powder with a particle size range of 0.3–0.5 mm. The RH powder was treated with a dilute NaOH solution to eliminate trace organic residues and then washed several times with deionized water at a pH of 6.0. The cleaned RH was dried at 80°C until a constant weight was obtained.

RH-*g*-GMA was synthesized by the graft copolymerization of GMA on the surface of the RH; this was initiated by $K_2S_2O_8$ in the presence of MBA (Figure 1). About 10 g of RH was immersed in 500 mL of an aqueous solution containing 0.5 g of MBA and 1.0 g of $K_2S_2O_8$. GMA (15 mL) and cyclohexane (15 mL) were added to this mixture, and the contents were stirred vigorously at 70°C for 4 h. After the completion of the reaction, the copolymerization product (RH-*g*-GMA) was filtered and washed thoroughly with deionized water and

methanol to remove the physically absorbed reactants and subsequently dried at 60°C.

The RH-*g*-GMA obtained as described previously was then subjected to an amination reaction to produce RH-*g*-GMA–Am (Figure 1). To conduct the amination reaction, the RH-*g*-GMA (5 g) was transferred into a glass bottle containing amines (20 mL), and the mixture was shaken at 150 rpm and 60–100°C, for a predetermined time (Figure S1). The obtained product was washed thoroughly with deionized water and finally dried at 60°C until a constant weight was achieved.

Characterization of the Native and Modified RH Samples

Scanning electron microscopy micrographs were used to observe the change in the surface morphology between RH and RH-*g*-GMA–Am. The chemical structures of RH, RH-*g*-GMA, and RH-*g*-GMA–Am were analyzed with Fourier transform infrared spectroscopy with an IR spectrophotometer (Shimadzu IR-435, Japan). The thermal decomposition behavior of the unmodified and modified RH samples was determined with a thermogravimetric analyzer (Mettler-Toledo TGA/DSC 1). All of the measurements were performed under a nitrogen atmosphere with a gas flow rate of 20 mL/min through the heating of the material from room temperature to 600°C at a heating rate of 10°C/min.

The surface charge of the RH samples was determined by a potentiometric titration method. The RH was mixed with a 0.01*M* $NaNO_3$ solution to obtain a suspension with an RH concentration of 2 g/L. The suspension was stirred with a magnetic stirrer while a temperature of 20 °C was maintained. Before the titration, the suspension was equilibrated until a pH value of 7.0 ± 0.1 was obtained. The titrations were performed by the addition of incremental volumes of 0.1*M* HNO_3 and 0.1*M* NaOH standard solutions to the suspension with a micropipette. The pH values of the suspensions were measured with a benchtop pH meter (Thermo Scientific Orion 3-Star). The surface charge density (σ; C/cm^2), was calculated with the following equation:

$$\sigma = \frac{F(C_A\text{-}C_B + [OH^-]\text{-}[H^+])}{WA} \quad (1)$$

where F is the Faraday constant (96,490 C/mol); C_A and C_B are the concentrations of the acid and base after each addition during the titration (mol/L), respectively; $[H^+]$ and $[OH^-]$ represent the equilibrium concentrations of the H^+ and OH^- ions, respectively; and W and A are the weight (g/L) and the surface area of the RH used (cm^2/g), respectively.

Sorption Experiments

The sorption experiments were carried out under batch conditions, where 0.1–0.2 g of the sorbent was added to 250-mL high-density polyethylene bottles containing 100 mL of an aqueous solution with known ion species and concentrations. The bottles were settled in an incubator shaker and continuously shaken at 25°C and 120 rpm for 2 h. After the predetermined sorption time, the solid and liquid phases were separated, and the anion concentrations in the liquid phase were measured. The initial and final anion concentrations in the liquid solutions were determined with UV spectrometry (Shimadzu UV-2401PC) and ion chromatography (Waters LC). The initial pH of the solutions was adjusted to the desired value by the addition of HCl or NaOH solutions. In the sorption selectivity experiments, acetate buffer was used as the matrix solution to maintain a constant pH value.

The sorption capacity (q; mg/g) was calculated with the following mass balance equation[19]:

$$q = \frac{V(C_0 - C)}{W} \quad (2)$$

where C_0 and C are the initial and equilibrium liquid-phase concentrations of the anions (mg/L), respectively; V is the volume of the solution (L); and W is the dry weight of the adsorbent used (g).

For the regeneration studies, the anion-adsorbed sorbent was regenerated with 0.1*M* HCl and then washed and dried at 60°C for 24 h. It was then reused for the adsorption experiments. The sorption and regeneration cycles were repeated five times.

RESULTS AND DISCUSSION

Preparation of the Aminated RH Sorbent

The graft copolymerization of RH with GMA was carried out with the application of the previously described procedures and the grafting density, which is the area of the active surface after grafting was found to be approximately 120–130% of the nongrafted RH. This grafted copolymer was then treated with DETA for amination. The effect of the reaction temperature for the amination of RH-*g*-GMA on the sorption was tested for nitrates to estimate the maximum sorption efficiency. As a result, a maximum adsorption efficiency was attained above 60°C (Figure S2, Supporting Information).

Similarly, the reaction time for amination above 4 h did not show any change in the improvement of the adsorption capacity of nitrates on the RH-*g*-GMA–Am surface (Figure S3). Therefore, the amination reaction for all of the experiments was maintained in the temperature range 60–100°C for 4 h.

Characterization of the Native and Modified RH

Adsorbent Morphology. A scanning electron microscopy picture was used to view the surface morphology change in RH before and after grafting. The two sides of RH were not the same. When the pictures were observed in magnified view, the outer side had a rough surface, whereas the inner side appeared to be smooth [Figure 2(a1,a2)]. In a comparison of both the outer and inner surfaces of RH and RH-*g*-GMA–Am, the latter had a much rougher surface; this indicated that the successful grafting of aminated GMA on the RH surface (Figure 2). According to the change in the morphology, it was possible to assume an increased adsorption site for anions when the amine groups were protonated.

IR Spectroscopy

The Fourier transform infrared spectra for the untreated RH, NaOH-pretreated RH, RH-*g*-GMA, and RH-*g*-GMA–Am are presented in Figure 3. In the case of untreated RH, a broad band ranging from 3100–3700 cm^{-1} was observed because of the hydroxyl groups (—OH ions) present in the cellulose fibers on the surface of RH. This broad peak was not affected by the pretreatment of the RH surface with NaOH. After grafting,

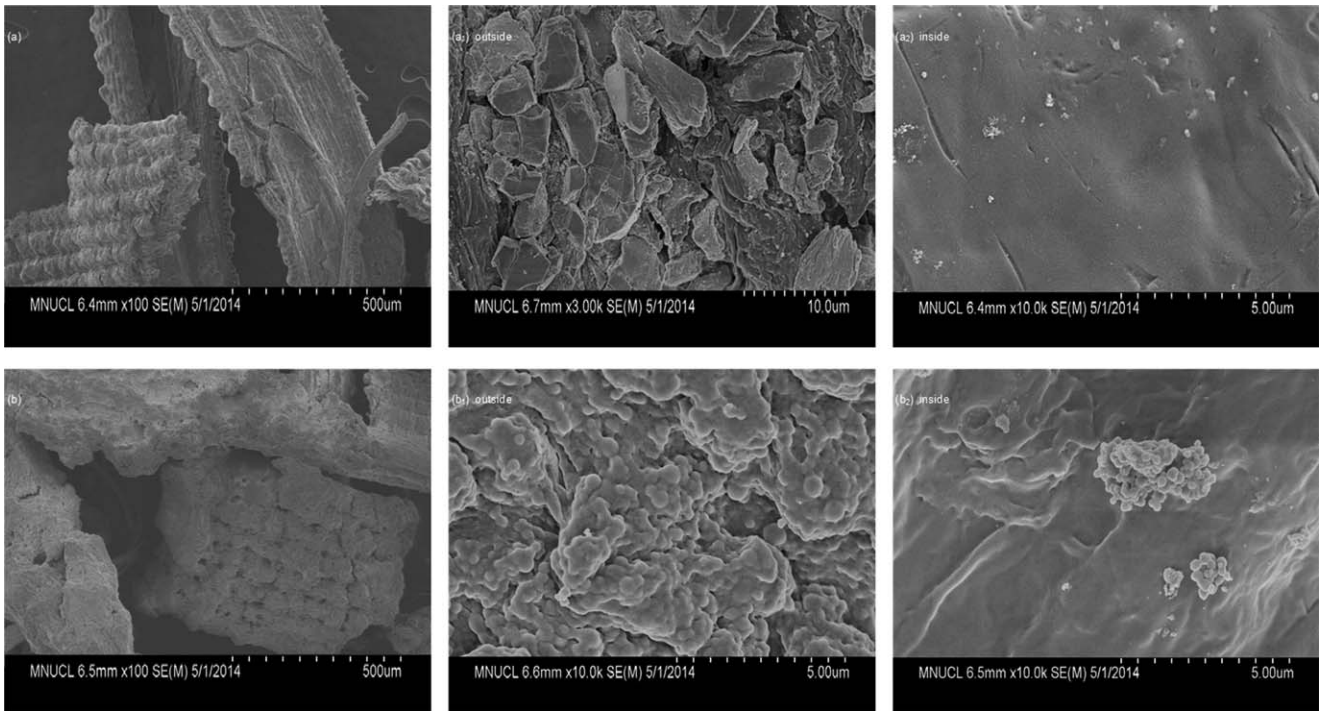

Figure 2. Scanning electron microscopy images of (a) raw RH and (b) RH-*g*-GMA–Am.

RH-*g*-GMA exhibited three new peaks at 1700 cm^{-1} (C═O stretching vibrations peak) and at 1500 and 1100 cm^{-1} (C—O symmetric and asymmetric vibrations in GMA). The peak around 2975 cm^{-1} was attributed to the vinyl groups in GMA. In addition, the double peak around 1453 and 1383 cm^{-1} corresponded to the stretching of the C—O groups in the carboxylates. The amination process produced some additional hydroxyl and —NH groups. The broad band ranging from 3100 to 3700 cm^{-1} in the spectrum was attributed to the overlapping of the stretching vibrations of both —OH and —NH groups. This newly formed and pronounced functional groups were assumed to improve the adsorption capacity of the adsorbent surface.

Thermogravimetric Analysis. Two stages of thermal decomposition were observed for RH-*g*-GMA and RH-*g*-GMA–Am, compared to the one stage observed for the unmodified RH. The two decomposition stages observed were an indication of the effect of graft copolymerization and the effect of the addition of the amine groups on the thermal property of the surface. As shown in Figure 4, the RH-*g*-GMA complex showed an improved thermal resistance, whereas RH-*g*-GMA–Am showed a lower thermal resistance compared to the unmodified RH. The improvement in the thermal resistance for RH-*g*-GMA was likely due to the presence of the epoxide group from GMA. Because the amine group exhibited a high reactivity toward the epoxide group, the loss of thermal resistance in the case of RH-*g*-GMA–Am could have been a result of the loss of the epoxide groups. Both RH-*g*-GMA and RH-*g*-GMA–Am had low amounts of residue, possibly because of the decomposition of lignin and other compounds during the grafting copolymerization process.

Surface Charge as a Function of pH. The effect of the solution pH on the adsorption properties of the unmodified RH, RH-*g*-GMA, and RH-*g*-GMA–Am is presented in Figure 5. The charge per unit area of the adsorbent surface showed a gradual decrease in all three adsorbents as the solution pH increased. This trend was related to the electrostatic interactions between the polymers and the anions in the basic solution. The points of zero charge (PZCs) for RH and RH-*g*-GMA–Am were at a

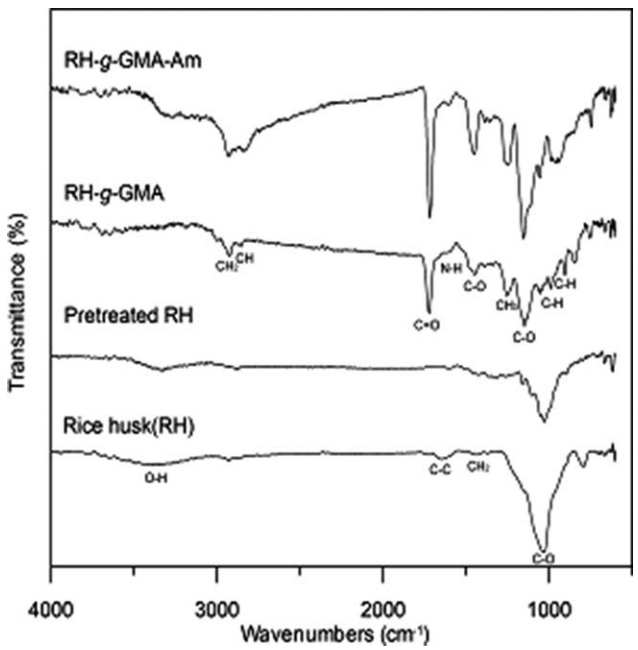

Figure 3. IR spectra of the untreated RH, RH pretreated with NaOH, RH-*g*-GMA, and RH-*g*-GMA–Am.

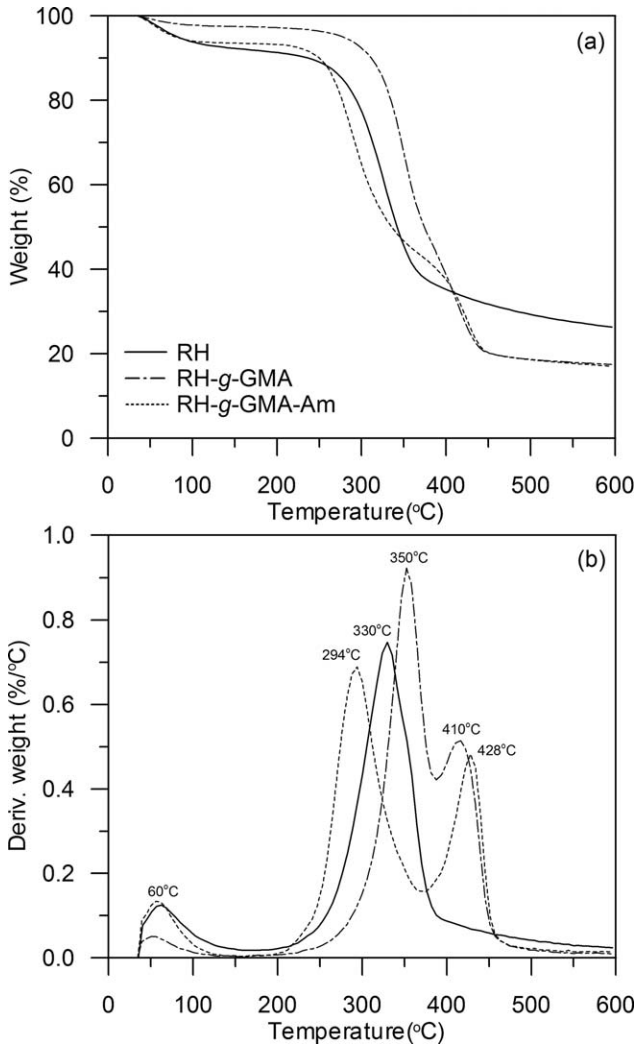

Figure 4. Comparison of the weight percentage changes on the thermal decomposition of the unmodified RH, RH-*g*-GMA, and RH-*g*-GMA–Am.

pH of 6, whereas the PZC for RH-*g*-GMA was at a pH of 7.4. The surface of RH-*g*-GMA–Am was positively charged at pH values below 6; this made it suitable for the adsorption of anions. For pH values above 6, because the amine groups were more prone to deprotonation and because the amount of positive charges on the surface decreased, the efficiency of anion adsorption subsequently decreased.

Adsorption Capability of the Modified and Unmodified RH. A comparison of the capacities of the unmodified RH, NaOH-pretreated RH, RH-*g*-GMA, and RH-*g*-GMA–Am to remove NO_3^- and PO_4^{3-} is presented in Figure 6(a). It is evident from the figure that for a given amount of sorbent and sorbate concentration (2 g/L and 1 mmol/L, respectively), the removal percentage for PO_4^{3-} was always higher than those of NO_3^- for all of the adsorbents because the charge concentration of the former was higher than that of the latter. However, the overall removal percentage for the two anions was much lower with the untreated RH, NaOH-pretreated RH, and RH-*g*-GMA compared to that for the RH-*g*-GMA–Am surface. The high sorption capability of RH-*g*-GMA–Am was attributed to the high level of interaction of the aminated surface with the anions. As presented in Figure 6(b), the choice of the reagent used for amination also greatly affects the sorption efficiency of the two anions for each sorbent. The surfaces aminated with TMA showed a lower sorption efficiency compared to the surfaces aminated with DETA, EDA or DMA. We noted that no significant difference was observed between the surfaces aminated with DETA and EDA. In comparison to the commercial ion-exchange resins SAR and WAR, except for the surface aminated with TMA, all of the other aminated surfaces showed better sorption efficiencies for PO_4^{3-}. However, for NO_3^-, the DETA, EDA, and DMA aminated surfaces showed comparable sorption capacities to that of SAR (40–50 mmol/g)and WAR. In summary, the results show that RH-*g*-GMA–Am, prepared with DETA, EDA, and DMA as the amination reagents had superior sorption capacities overall compared to the commercially available SAR and WAR anion-exchange resins.

Sorption Isotherms

The equilibrium sorption isotherms corresponding to the sorption of 2.0 g/L NO_3^- and 1.0 g/L PO_4^{3-} anions on the RH-*g*-GMA–Am surfaces prepared with 0.2–2.0 m*M* of DETA are shown in Figure 7(a). The experimentally determined data were fitted to three theoretical isotherm models, namely, the Langmuir, Freundlich, and Dubinin–Radushkevich isotherm models.

Langmuir Adsorption Isotherm. The Langmuir adsorption isotherm model mathematically describes the adsorption of a monolayer on an adsorbent surface and assumes that the adsorption is limited once all of the surface sites are occupied. The model assumes uniform energies of adsorption for all of the sites on the surface and no transmigration of the adsorbate in the surface plane.[10,11,20] The Langmuir isotherm model is represented by eq. (3):

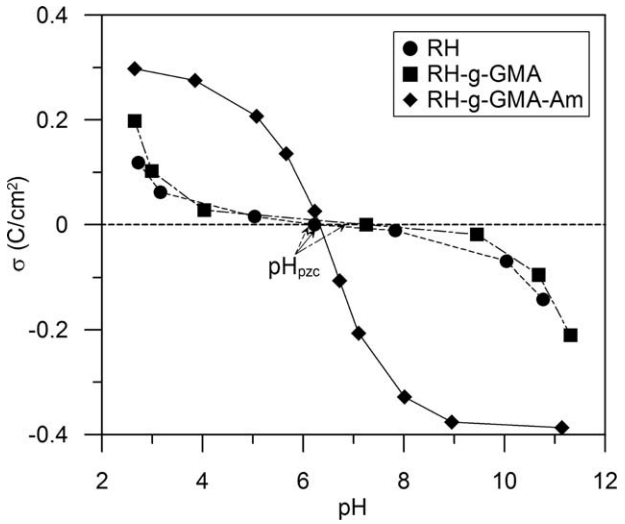

Figure 5. Effect of pH on the surface charge of the unmodified RH, RH-*g*-GMA, and RH-*g*-GMA–Am.

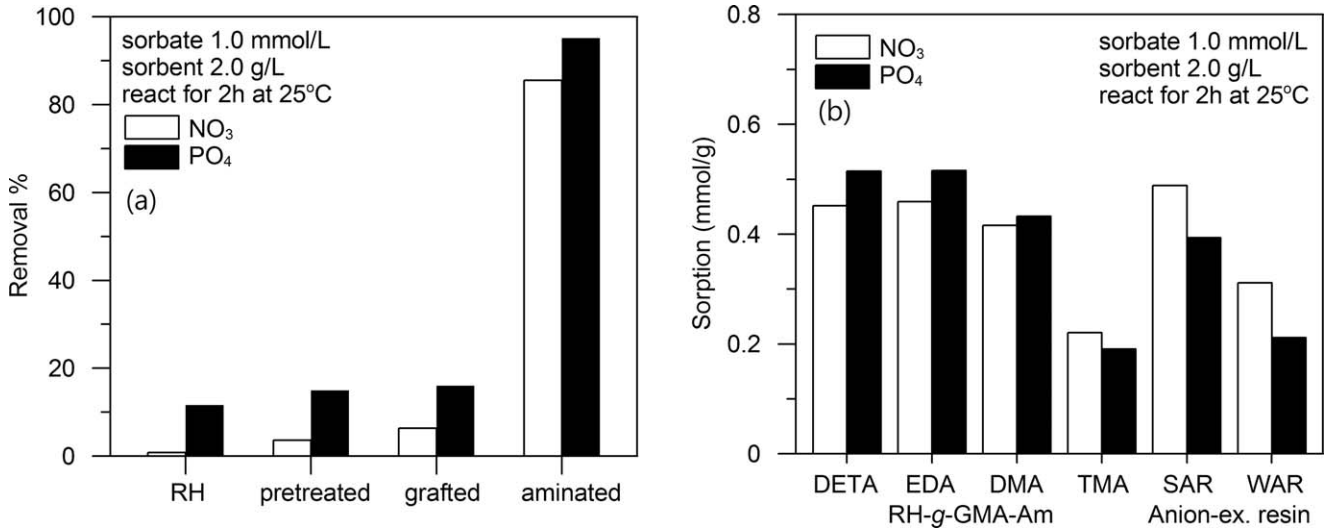

Figure 6. Comparison of the adsorption capacities of the (a) unmodified RH, RH-*g*-GMA, and RH-*g*-GMA–Am and (b) RH-*g*-GMA–Am prepared with various amination reagents and two commercially available anion-exchange resins.

$$q_e = \frac{Q_0 b C_e}{1 + b C_e} \tag{3}$$

where C_e is the equilibrium concentration of the adsorbate (mg/L), q_e is the amount of anion adsorbed per gram of adsorbent at equilibrium (mg/g), Q_o is the maximum monolayer coverage capacity (mg/g), and b is Langmuir isotherm constant (L/mg).

The values of Q_o and b computed from the slope and intercept of the Langmuir plot are tabulated in Table I. The data from the experiments revealed that the maximum sorption capacities for NO_3^- and PO_4^{3-} on RH-*g*-GMA–Am were 68.5 and 129.8 mg/g, respectively. The higher adsorption of PO_4^{3-} compared to NO_3^- may have been associated with the high electronegativity of the former compared to the latter. The linear fit of the experimental data to the Langmuir model exhibited a correlation coefficient of 0.997, and the *b*s were found to be 0.08 and 0.39 for NO_3^- and PO_4^{3-}, respectively.

Freundlich Adsorption Model. This model is usually used to mathematically model heterogeneous surfaces[10,18,20] and is represented by eq. (4):

$$Q_e = K_f C_e^{\frac{1}{n}} \tag{4}$$

where K_f is the Freundlich isotherm constant {(mg/g)[(L/mg)$^{1/n}$]}, n is the adsorption intensity, and Q_e is the amount of adsorbed anions on the adsorbent at equilibrium (mg/g).

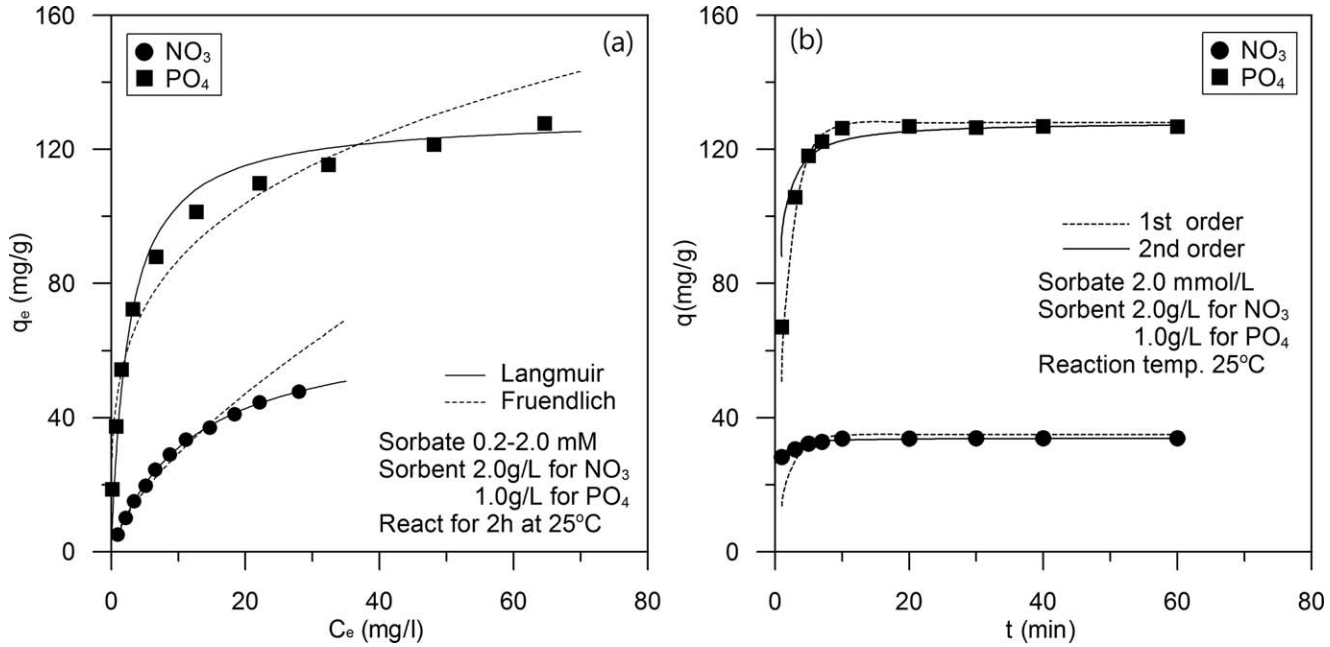

Figure 7. (a) Equilibrium sorption isotherms for the sorption of NO_3^- and PO_4^{3-} on RH-*g*-GMA–Am and (b) kinetics of adsorption of NO_3^- and PO_4^{3-} on RH-*g*-GMA–Am.

Table I. Langmuir, Freundlich, and Dubinin–Radushkevich Isotherm Parameters

	Langmuir isotherm			Fruendlich isotherm			Dubinin–Radushevich isotherm		
Anion	q_e (mg/g)	b (L/mg)	r^2	K_f [(mg/g) (L/mg)$^{1/n}$]	n	r^2	ε (kJ/mol)	q_m (mol/g)	r^2
NO_3^-	68.5	0.08	0.997	1.98	1.46	0.984	9.283	0.0071	0.991
PO_4^{3-}	129.8	0.39	0.997	1.29	2.34	0.945	140.06	0.0047	0.984

r correlation coefficient.

The values of K_f and $1/n$, which are indicators of the adsorption capacity and the strength of the adsorption process, respectively, are presented in Table I. The K_f values for NO_3^- and PO_4^{3-} were determined to be 1.98 and 1.29, respectively, whereas the n values are 1.46 and 2.34 for NO_3^- and PO_4^{3-}, respectively. Because the value of $1/n$ was below 1, it indicated a normal adsorption. The correlation coefficients for the fitting of the experimental data to the Freundlich isotherm were found to be 0.984 and 0.945 for NO_3^- and PO_4^{3-}, respectively.

Dubinin–Radushkevich Isotherm. The Dubinin–Radushkevich isotherm is generally applied to heterogeneous surfaces and is expressed with a Gaussian energy distribution.[20] The model is mathematically represented by the following equation:

$$q_e = q_s e^{(-K_{ad}\varepsilon^2)} \quad (5)$$

where q_s is the theoretical isotherm saturation capacity (mg/g) and K_{ad} (mol^2/kJ^2) and ε are the Dubinin–Radushkevich isotherm constants.

The linear fit of the experimental data to the Dubinin–Radushkevich isotherm yielded correlation coefficients of 0.991 and 0.984 for NO_3^- and PO_4^{3-}, respectively, and the maximum amounts of adsorbate on the adsorbent surface were found to be 0.0071 mol/g for the former and 0.0047 mol/g for the latter.

A comparison of the correlation coefficients for the fit of the experimental data to the three isotherm models revealed that the Langmuir isotherm model provided the best fit; this indicated the predominance of monolayer adsorption.

Sorption Kinetics

Understanding of the sorption kinetics is important for selecting the optimum operating conditions for developing a full-scale batch process. The kinetics of the adsorption of NO_3^- and PO_4^{3-} on RH-*g*-GMA–Am were studied, and the results are presented in Figure 7(b). For the range of NO_3^- and PO_4^{3-} concentrations studied, the uptake of both anions was rapid during the first 7 min. After 7 min, the rapid uptake decelerated, and a much slower second adsorption step followed. This initial rapid uptake was related to the concentration gradient between the adsorbate concentration in the solution and that on the RH-*g*-GMA–Am surface present at the beginning of the adsorption process. As the concentration of the adsorbate on the adsorbent surface increased, the concentration gradient decreased; this led to a slower uptake of the adsorbate, and eventually, an equilibrium was attained. The experimental data were fitted with the pseudo-first-order and pseudo-second-order kinetic models, and the rate constants (K_1 and K_2) and correlation coefficients were determined, as shown in Table II. From the values in the table, we concluded that the pseudo-second-order kinetic equation represented the adsorption process better than the pseudo-first-order kinetics equation. Furthermore, from Figure 7, we inferred that chemisorption was likely the rate-determining step.

Macropore and Micropore Diffusion

The adsorption mechanism of a sorbate onto a sorbent surface follows three steps, namely, film diffusion, pore diffusion, and intraparticle transport. The slowest of the three steps controls the overall rate of the process.[21] In most batch-operated processes, the rate-limiting steps are pore diffusion and intraparticle transport. Oladoja *et al.* (2008) cited refs. 8 and [22] and reported that in a batch process, although there was a high possibility for pore diffusion to be the rate-limiting step, the rate parameter for intraparticle diffusion mostly controlled the overall process time. The widely used equation for a sorption system is given by eq. (6):

$$q_t = k_i t^{0.5} \quad (6)$$

where k_i is the intraparticle rate constant (mg/g min$^{0.5}$). From the plot of q versus $t^{0.5}$, as shown in Figure 8, the slope k_i was determined and tabulated in Table III. A decrease in the pore size and a reduction in the free path with possible pore blockage resulted in a dramatic reduction in the diffusion parameters.[8] Because of these effects, the process, as shown in Figure 8, had two consecutive linear segments with slopes of $k_{id,1}$ and $k_{id,2}$.

Table II. Pseudo-First- and Second-Order Kinetic Parameters

	Experiment	Pseudo-first-order kinetics[a]		Pseudo-second-order kinetics		
Anion	q_e (mg/g)	K_1 (min^{-1})	r^2	K_2 (g/mg min)	q_e (mg/g)	r^2
NO_3^-	33.8	0.498	0.919	0.147	34.0	1.000
PO_4^{3-}	126.8	0.507	0.994	0.016	128.2	0.999

[a] Only for the initial sorption period (0–7 min).

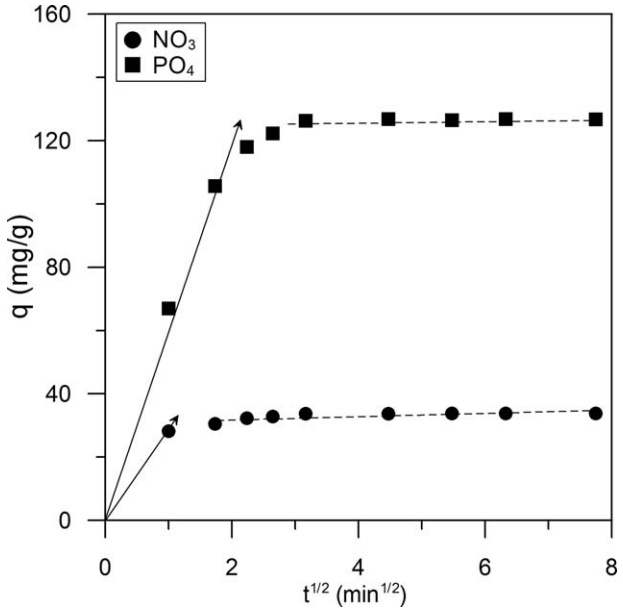

Figure 8. Intraparticle and pore diffusion plots for the adsorption of NO_3^- and PO_4^{3-} on RH-*g*-GMA–Am.

Therefore, with the results in Table III, the slope of the first linear part ($k_{id,1}$) was relatively high compared to those of the second linear part. This indicated that the mass transfer in the first part, which was shorter, occurred as a result of the boundary layer diffusion, and for the second part, where the limiting time for the process was recorded, the slope of the second linear part ($k_{id,2}$) was reduced considerably; this showed that the pores were micropores and that intraparticle diffusion occurred.

Regeneration Efficiency

The regeneration tendency of an adsorbent surface was a basic property that is often considered in choosing the most convenient, cost-effective, and environmentally friendly adsorbent. For RH-*g*-GMA–Am, a repetitive regeneration experiment for five cycles was conducted with 0.1*N* HCl, and the results are presented in Figure 9. As the number of regeneration cycles increased, RH-*g*-GMA–Am lost weight [Figure 9(b)]; this resulted in the loss of some active sites. The loss in active sites was corroborated by the observation that the amount of NO_3^- adsorbed on the RH-*g*-GMA–Am surface decreased with increasing number of regeneration cycles.

Table III. Intraparticle Diffusion Model Parameters

	First linear portion			Second linear portion		
Anion	$k_{id,1}$(mg/g min$^{0.5}$)	q_1 (mg/g)	r^2	$k_{id,2}$ (mg/g min$^{0.5}$)	q_2 (mg/g)	r^2
NO_3^-	28.20	0. 00	1.000	2.19	27.00	0.962
PO_4^{3-}	61.38	1.67	0.996	8.94	98.26	0.993

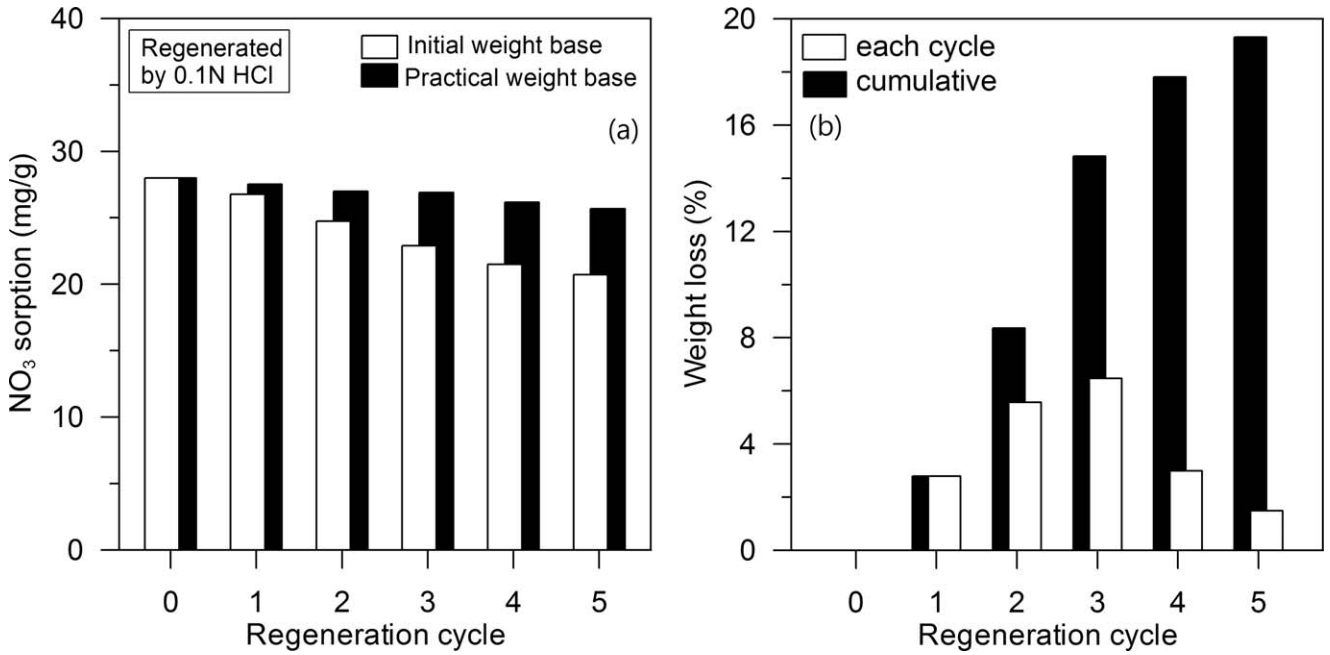

Figure 9. Effect of regeneration on the adsorption surface: (a) adsorption capacity of NO_3^- as a function of the number of regeneration cycles of the adsorbent and (b) weight loss of the adsorbent as a function of the number of regeneration cycles.

CONCLUSIONS

In this study, we synthesized RH-*g*-GMA–Am and examined its efficiency as an adsorbent for anions, such as NO_3^- and PO_4^{3-}, which are common pollutants in wastewater. RH-*g*-GMA–Am was produced by the amination of RH-*g*-GMA with DETA as the amination reagent. The results of the study clearly show that RH-*g*-GMA–Am improved the surface adsorption properties compared to the monomers used. The introduction of amine groups on RH-*g*-GMA increased the net positive charge on the surface and, thereby, improved the anion adsorption at acidic pH values below 6. Furthermore, the experimental sorption data fit best with the Langmuir model; this suggested the predominance of monolayer adsorption. The sorption kinetics data for both NO_3^- and PO_4^{3-} removal showed that the adsorption process was a result of two consecutive processes. The adsorption process was found to follow the pseudo-second-order kinetic model, which is rate-limited by chemisorption. The amination of RH-*g*-GMA to form RH-*g*-GMA–Am drastically improved the adsorption efficiency of NO_3^- and PO_4^{3-} from 3 to 82% and from 6 to 93%, respectively. The aminated surface showed a high removal efficiency for PO_4^{3-} at pH values above 4.5. Finally, the regeneration efficiency of the RH-*g*-GMA–Am surface was studied for five cycles; this showed that the surface of RH-*g*-GMA–Am was regenerated repetitively by simple acid washing with an insignificant decrease in the active surface for subsequent adsorptions.

ACKNOWLEDGMENTS

This research was supported by the Basic Science Research Program through the National Research Foundation of Korea, which was funded by the Ministry of Education, Science, and Technology (contract grant number 2015052334).

REFERENCES

1. Loganathan, P.; Vigneswaran, S.; Kandasamy, J. *J. Environ. Manage.* **2013**, *131*, 363.
2. Xu, X.; Gao, B.; Yue, Q.; Li, Q.; Wang, Y. *Chem. Eng. J.* **2013**, *234*, 397.
3. Lu, J.; Liu, H.; Zhao, X.; Jefferson, W.; Cheng, F.; Qu, J. *Colloids Surf. A* **2014**, *455*, 11.
4. Jal, P. K.; Patel, S.; Mishra, B. K. *Talanta* **2004**, *62*, 1005.
5. Park, H.-J.; Na, C.-K. *J. Colloid Interface Sci.* **2006**, *301*, 46.
6. Deng, S.; Niu, L.; Bei, Y.; Wang, B.; Huang, J.; Yu, G. *Chemosphere* **2013**, *91*, 124.
7. Xu, M.; Yin, P.; Liu, X.; Tang, Q.; Qu, R.; Xu, Q. *Bioresour. Technol.* **2013**, *149*, 420.
8. Allen, S. J.; McKay, G.; Khader, K. Y. H. *Environ. Pollut.* **1989**, *56*, 39.
9. Bhattacharya, A.; Rawlins, J. W.; Ray, P. Polymer Grafting and Crosslinking; Wiley: Hoboken, NJ, **2008**.
10. Park, H.-J.; Na, C.-K. *J. Hazard. Mater.* **2009**, *166*, 1201.
11. Song, X.-J.; Hu, J.; Wang, C.-C. *Colloids Surf. A* **2011**, *380*, 250.
12. Gao, B.; Lei, H.; Jiang, L.; Zhu, Y. *J. Chromatogr. B* **2007**, *853*, 62.
13. Yang, G.; Chen, H.; Qin, H.; Feng, Y. *Appl. Surf. Sci.* **2014**, *293*, 299.
14. Pan, B. C.; Xiong, Y.; Su, Q.; Li, A. M.; Chen, J. L.; Zhang, Q. X. *Chemosphere* **2003**, *51*, 953.
15. Orlando, U. S.; Baes, A. U.; Nishijima, W.; Okada, M. *Chemosphere* **2002**, *48*, 1041.
16. Gupta, V. K.; Suhas, J. *Environ. Manage.* **2009**, *90*, 2313.
17. Bhatnagar, A.; Sillanpää, M. *Chem. Eng. J.* **2011**, *168*, 493.
18. Hwang, C. W.; Kwak, N.-S.; Hwang, T. S. *Chem. Eng. J.* **2013**, *226*, 79.
19. Bayramoglu, G.; Yavuz, E.; Senkal, B. F.; Arica, M. Y. *Colloids Surf. A* **2009**, *345*, 127.
20. Dada, A. O.; Olalekan, A. P.; Olatunya, A. M.; Dada, O. *IOSR J. Appl. Chem.* **2012**, *3*, 38.
21. Goswami, S.; Ghosh, U. C. *Water SA* **2005**, *31*, 5.
22. Weber, W. J.; Morris, J. C. *J. Sanitary Eng. Div. Am. Soc. Civil Eng.* **1963**, *89*, 31.